

Title	Study on bone quality in the human mandible- Alignment of biological apatite crystallites
Author(s) Alternative	Furukawa, T; Matsunaga, S; Morioka, T; Nakano, T; Abe, S; Yoshinari, M; Yajima, Y
Journal	Journal of biomedical materials research. Part B, Applied biomaterials, 107(3): 838-846
URL	http://hdl.handle.net/10130/5136
Right	This is the peer reviewed version of the following article: J Biomed Mater Res B Appl Biomater. 2019 Apr;107(3):838-846, which has been published in final form at https://doi.org/10.1002/jbm.b.34180 . This article may be used for non-commercial purposes in accordance with Wiley Terms and Conditions for Use of Self-Archived Versions.
Description	

Title: Study on bone quality in the human mandible -Alignment of biological apatite crystallites-

Takehiro Furukawa^{1) 2)}, Satoru Matsunaga^{1) 3)}, Toshiyuki Morioka^{1) 4)}, Takayoshi Nakano⁵⁾, Shinichi Abe³⁾, Masao Yoshinari¹⁾, Yasutomo Yajima^{1) 2)}

1) Oral Health Science Center, Tokyo Dental College, Tokyo, Japan

2) Department of Oral and Maxillofacial Implantology, Tokyo Dental College, Tokyo, Japan

3) Department of Anatomy, Tokyo Dental College, Tokyo, Japan

4) Department of Removable Partial Prosthodontics, Tokyo Dental College, Tokyo, Japan

5) Division of Materials & Manufacturing Science, Graduate School of Engineering, Osaka University, Osaka, Japan

Running Heads: Alignment of BAp crystallites in cortical bone of human mandible

Abstract

Introduction: The importance of considering bone quality during oral implant treatment is increasingly being recognized. Assessment of bone quality in response to changes in the jaw bone is extremely important when planning treatment. The present study analyzed BAp crystallites, a bone quality factor, in order to investigate crystallographic anisotropy in dentate and edentulous human mandibles.

Materials and Methods: Using mandibular samples from Japanese adult cadavers, a region of interest was established comprising cortical bone in the central incisors. Samples were classified into five morphological categories based on the extent of bone resorption. BMD was measured and diffraction intensity ratios were calculated using a microbeam X-ray diffraction system.

Results: While no differences were observed in BMD, differences were observed in BAp crystallite alignment between the measurement points. In the alveolar region, samples with residual alveolar bone showed strong alignment in occlusal direction, while samples with marked alveolar bone resorption had preferential alignment in the mesiodistal direction.

Conclusion: The present findings suggest that tooth loss and the extent of alveolar bone resorption affects bone quality in the mandible.

Keywords:

Human mandible, Biological apatite crystallite, Bone quality, Microbeam X-ray diffraction, Bone mineral density

1. Introduction

Oral implant treatment has recently become a popular prosthetic approach for tooth loss. With an overall implant survival rate of 96.3%, Jung et al.¹ reported particularly high survival rates for mandibular compared to maxillary dental implants. Conversely, Bruno et al.² attributed oral implant treatment failure to insufficient bone quality in addition to systemic disease and environmental conditions. Alsaadi et al.³ suggested that bone quality may affect successful osseointegration, reporting decreased bone quality as a local factor for early implant loss.

At the 2000 National Institutes of Health Consensus Development Conference, bone quality was proposed as an important factor affecting bone strength. Improved bone quality is likely to increase bone strength and thereby implant success rate.⁴ Bone quality parameters include bone metabolism and microstructure and the presence of microcracks. Among these factors, biological apatite (BAp) crystallites are highly resistant to compressive loads; therefore, increasing focus is being given to the use of BAp crystallite alignment analysis to accurately predict the mechanical environment.^{5,6,7,8} BAp crystallites have a highly anisotropic hexagonal ionic structure with a high Young's modulus in their preferential alignment direction.⁷ Nakano et al.⁸ evaluated BAp crystallite alignment in animal ulna, parietal bone, and mandible and reported differences in mechanical function in each bone type. Recent studies have shown that the preferential alignment of BAp crystallites in the human dentate mandible differs between the alveolar region and the base of the mandible.^{9,10,11} However, many details remain to be clarified regarding structural anisotropy and the mechanical environment of the alveolar region in the human mandible. Bone

resorption is accompanied by tooth loss from the alveolar region of the human mandible, resulting in marked changes in both bone strength and structural characteristics, as well as external appearance.^{12,13} Prior to oral implant treatment, it is particularly important to obtain qualitative data regarding the affected jaw bone and to consider the nerves and arteries running through and around the bone in accordance with bone resorption volume and implant site.¹⁴ In the McGill consensus statement, oral implant treatment in the anterior region was proposed as being effective for edentulous mandible.¹⁵ Evaluation of bone quality is essential in order to achieve more accurate oral implant treatment. The present study aimed to clarify the structural anisotropy in the human dentate and edentulous mandible by quantitatively evaluating bone quality.

2. Materials and Methods

2.1 Samples

Samples were extracted from 15 Japanese adult cadavers (mean age, 73.4 ± 17.4 years; 10 male and 5 female), from the collection at the Department of Anatomy, Tokyo Dental College. The present study was approved by the Ethics Committee of Tokyo Dental College (Ethics Application No. 783). Edentulous mandibles without extraction sockets from mouths and complete maxillary and mandibular were used. As controls, dentate mandibles were used. The harvested mandibles were divided into five morphological categories based on those used by Atwood¹⁶: A) dentate mandible; B) edentulous mandible with high, well-rounded alveolar region (time since tooth extraction: ≤ 6 months, 6 months–2 years); C) edentulous mandible with high, knife-edge alveolar region (2–20 years); D) edentulous mandible with

low, well-rounded alveolar region (≥ 20 years); and E) edentulous mandible with low, depressed alveolar region (≥ 20 years) with three samples in each category (Fig. 1-A). Further, the morphological categories were grouped into dentate samples (group α ; A), and edentulous samples with residual alveolar bone (group β ; B, C) or marked alveolar bone resorption (group γ ; D, E). The midline was defined as the mesioproximal surface of the mandibular central incisors in the dentate mandible and the center of the mental spine in the edentulous mandible. The region of interest in the dentate mandible was established as a sagittal cross section of the mandibular plane passing vertically through the axis of the mandibular central incisor. In the edentulous mandible, the region of interest comprised a vertical section of the mandibular plane 2.75 mm from the midline at the central point of the mesiodistal width of Japanese adult mandibular central incisors (Fig. 2).

After fixation in 10% formalin and ethanol dehydration, samples were embedded in autopolymerizing acrylic resin and sagittally sectioned using a saw microtome with a blade width of 300 μm (SP1600; Leica, Wetzlar, Germany). Samples were then sanded to a thickness of 200 μm using wet/dry sandpaper of increasing grit (#400, #800, and #1200).

2.2 Micro-computed tomography (micro-CT) scan

Micro-CT (HMX225 Actis4; Tesco Corporation, Tokyo, Japan) was performed to examine sample macrostructure under the following imaging conditions: tube voltage, 140 kV; tube current, 100 μA ; matrix size, 512 \times 512; magnification, $\times 2.5$; slice width, 50 μm ; and slice pitch, 50 μm . A region of interest was established from alveolar crest to the base of the mandible. Three-dimensional structural analysis was performed using TRI/3D-BON

software (RATOC System Engineering, Tokyo, Japan).

2.3 Measurement sites

Measurements in the alveolar region were made at the following four points in the cortical bone at the stated distance below the alveolar crest: I, 8 mm on the labial side; II, 4 mm on the labial side; III, 4 mm on the lingual side; and IV, 8 mm on the lingual side. In the base of the mandible, measurements were made at the following four points in the cortical bone at the stated distance above the inferior border of the mandible: V, 8 mm on the labial side; VI, 4 mm on the labial side; VII, 4 mm on the lingual side; and VIII, 8 mm on the lingual side (Fig. 1-B).

2.4 Bone mineral density (BMD)

BMD was measured using micro-CT depicting the same area as the regions of interest defined above. Epoxy resin phantoms ($\phi 6 \times 1$ mm) containing hydroxyapatite were used. Phantom densities were as follows: 800 mg/cm³, 700 mg/cm³, 600 mg/cm³, 500 mg/cm³, 400 mg/cm³, 300 mg/cm³, and 200 mg/cm³. Based on the calibration curve created by micro-CT imaging of the phantoms, BMD of points I–VIII were calculated for each sample using TRI/3D-BON-BMD-PNTM2 software (RATOC System Engineering, Tokyo, Japan).

2.5 Biological apatite (BAp) crystallite alignment

Quantitative analysis of BAp crystallite alignment was conducted using an optical curved imaging plate (IP) X-ray diffraction system (XRD; D/MAX RAPID II-CMF; Rigaku

Corporation, Tokyo, Japan). Measurements were performed in reflection and transmission modes with Cu-K α as the radiation source at a tube voltage of 40 kV and tube current of 30 mA. Reference axes were established in the mesiodistal (X axis), occlusal (Y axis), and labiolingual (Z axis) directions for each sample (Fig. 3). The radiation site was determined using the light microscope (magnification, $\times 0.6$ –4.8). An incident beam with a diameter of 100 μm was applied, centered on the interstitial lamella surrounding the osteon. Reflection mode was used in the X axis and transmission mode in the Y and Z axis directions, respectively, and the diffracted X-ray beam was detected using a curved IP based on the conditions described by Nakano et al.⁸

The diffracted X-ray beam was detected as a diffraction ring on the IP. Using 2D Data Processing software (Rigaku Corporation, Tokyo, Japan), X-ray diffraction intensity ratios were calculated for the two diffraction peaks corresponding to planes 002 and 310. Calculations were performed three times at each measurement point and the mean X-ray diffraction intensity ratio was used as the calculated value.

2.6 Statistical analysis

Differences between the morphological categories regarding the alveolar region and the base of the mandible were analyzed using one-way analysis of variance followed by Tukey's multiple comparison test. In addition, a t-test was used to compare the alveolar region and the base of the mandible. Significance was set at $P < 0.05$.

3. Results

3.1 BMD

BMD at each measurement point are shown in table 1. BMD for each category (A–E) are evaluated using the mean values for measurement points I–IV and V–VIII, respectively (Fig. 4). No significant differences were observed in BMD between the alveolar region and the base of the mandible or between categories A–E.

3.2 BAp crystallite alignment

The X-ray diffraction intensity ratios on the X axis at each measurement point are shown in table 2. The X-ray diffraction intensity ratios on the X axis for each category (A–E) are evaluated using the mean values for measurement points I–IV and V–VIII, respectively (Fig. 5). In the alveolar region, significantly lower intensity ratios (indicating a low degree of BAp crystallite alignment) were noted on the X axis in the categories with residual alveolar bone (A–C) compared to those with marked alveolar bone resorption (D and E). Conversely, no significant differences were observed between the categories in the base of the mandible.

The X-ray diffraction intensity ratios on the Y axis at each measurement point are shown in table 3. The X-ray diffraction intensity ratios on the Y axis for each category (A–E) are evaluated using the mean values for measurement points I–IV and V–VIII, respectively (Fig. 6). In the alveolar region, significantly higher intensity ratios (indicating a high degree of BAp crystallite alignment) were noted in the categories with residual alveolar bone compared to those with marked resorption. In the base of the mandible, significant differences were observed between categories A and C, and B and E; however, overall intensity ratios were low.

The X-ray diffraction intensity ratios on the Z axis at each measurement point are shown in table 4. The X-ray diffraction intensity ratios on the Z axis for each category (A–E) are evaluated using the mean values for measurement points I–IV and V–VIII, respectively (Fig. 7). Overall X-ray diffraction intensity ratios were low and while significant differences were observed between categories A and B, and A and E in the alveolar region, no significant differences were observed in the base of the mandible.

The X-ray diffraction intensity ratios are compared between the alveolar region and the base of the mandible in each group (Fig. 8). In groups α and β , uniaxial preferential alignment was noted on the X axis in the base of the mandible and on the Y axis in the alveolar region. No anisotropic BAp crystallite alignment was shown in group γ .

4. Discussion

4.1 BMD

Many studies have been published regarding BMD in the jaw bones; however, results vary depending on the measurement method and site. Previous study have reported that BMD in human edentulous jaw bones differs depending on the bone region, with the highest values found in the anterior mandible.^{17,18} However, the present study showed no significant differences in BMD between the alveolar region and the base of the mandible, regardless of the extent of alveolar bone resorption. This is consistent with the recent study.¹⁰ Thus, localized bone evaluation based solely on BMD is clearly problematic.

4.2 BAp crystallite alignment

A high degree of preferential alignment in the occlusal (Y axis) direction was shown in dentate mandibles and in the alveolar region with residual alveolar bone in edentulous mandibles. As the extent of bone resorption increased in this region, preferential alignment in the occlusal direction significantly decreased. In experiments on monkey mandibles, the c axis of BAp crystallites was aligned along the long axis in the mesiodistal direction but in the vicinity of the teeth, alignment changed to the direction of occlusal pressure.⁸ It is also reported preferential alignment in the occlusal direction in the alveolar region in the anterior tooth of the human dentate mandible.¹⁰ The results of the present study regarding dentate mandibles and edentulous mandibles with residual alveolar bone are consistent with the findings of these previous studies. Therefore, the differences in BAp crystallite alignment observed in the present study may be attributable to the mandible becoming less sensitive to mechanical stress due to tooth loss or alveolar bone resorption and subsequent loss of homeostasis.

The presence or absence of dentition had a greater effect on mandibular alveolar bone resorption than aging or sex.¹⁹ Furthermore, animal experiments decreased alveolar bone osteogenesis and mechanical properties with decreased occlusal function.²⁰ The low values in alignment of BAp crystallites in the alveolar regions of edentulous jaws with marked alveolar bone resorption observed may be attributable to reduced mechanical stress after tooth loss.

Odaka et al. compared BAp crystallite alignment before and after implant placement in the peri-implant bone region in beagles and reported a high degree of preferential alignment in the direction of load transmission surrounding implant.²¹ Meanwhile, Nakano et al.

analyzed bone quality during post-fracture bone healing and found that recovery of Young's modulus strongly correlated with increased BAp crystallite alignment rather than with BMD.^{22,23} In the present study, the degree of BAp crystallite alignment in the occlusal direction was high in samples with residual alveolar bone even after tooth loss and low in samples with marked alveolar bone resorption. As drilling during dental implant placement involves bone destruction, post-implant healing is comparable to that after bone fracture.^{24,25} Since it was reported at the 4th International Team for Implantology Consensus Conference that conventional implant loading should be performed at least 2 months after implant placement, this timing has been widely adopted in clinical practice.²⁶ In patients with residual alveolar bone, bone quality is maintained and rapidly reaches optimal status after implant placement. Conversely, in patients with marked alveolar bone resorption, bone quality becomes worse in addition to bone density and bone recovery is likely to require more time. Therefore, in patients with marked alveolar bone resorption, the implant placement method and load condition and timing should be carefully decided.

Findings in the present study regarding alignment in the mesiodistal direction were consistent with the present study, with strong alignment in the alveolar region correlating with greater bone resorption.²⁷ This is thought to result from acquisition of preferential alignment in the mesiodistal direction in the form of new long bone following loss of preferential alignment in the occlusal direction in the edentulous mandible.

5. Conclusion

The results of the present study clarified that marked alveolar bone resorption causes

loss of not only bone density, but also BAp crystallite alignment in the alveolar region. In the face of marked alveolar bone resorption, deterioration of bone quality factors means that the role of alveolar bone in providing tooth support is likely to be lost even if bone density is retained. Even with local osteogenesis after implant placement, more time will be required for optimization of bone quality to be reached. Therefore, in patients with marked alveolar bone resorption, implant placement method and load condition and timing should be carefully decided.

Acknowledgements

This research was supported by a Grant-in-Aid for Scientific Research (C) (17K11808 and 25463055) from the Japan Society for the Promotion of Science. The authors would like to thank Mrs. Eiko Watanabe for her technical assistance.

Conflict of interest

The authors declare that there is no conflict of interest.

REFERENCES

1. Jung RE, Zembic A, Pjetursson BE, Zwahlen M. Systematic review of the survival rate and the incidence of biological, technical, and aesthetic complications of single crowns on implants reported in longitudinal studies with a mean follow-up of 5 years. *Clin Oral Implants Res* 2012; 23: 2–21.
2. Chrcanovic BR, Kisch J, Albrektsson T, Wennerberg A. Analysis of risk factors for cluster behavior of dental implant failures. *Clin Implant Dent Relat Res* 2017: 1–11.
3. Alsaadi G, Quirynen M, Komárek A, Steenberghe DV. Impact of local and systemic factors on the incidence of oral implant failures, up to abutment connection. *J Clin Periodontol* 2007; 34: 610–617.
4. NIH consensus development panel on osteoporosis prevention, diagnosis, and therapy. *JAMA* 2001; 285: 785–795.
5. Sasaki N, Sudoh Y. X-ray pole figure analysis of apatite crystals and collagen molecules in bone. *Calcif Tissue Int* 1997; 60: 361–367.
6. Sasaki K, Nakano T, Ferrara JD, Lee JW, Sasaki T. New technique for evaluation of preferential alignment of Biological Apatite (BAp) crystallites in bone using transmission X-ray diffractometry. *Mater Trans* 2008; 49: 2129–2135.
7. Elliot JC. Structure and chemistry of the apatites and other calcium orthophosphates. Elsevier Sci Amsterdam 1994: 1–389.
8. Nakano T, Kaiba K, Tabata Y, Nagata N, Enomoto S, Marukawa E, Umakoshi Y. Unique alignment and texture of biological apatite crystallites in typical calcified tissues analyzed by microbeam X-ray diffractometer system. *Bone* 2002; 31: 479–

487.

9. Morioka T, Matsunaga S, Yoshinari M, Ide Y, Nakano T, Sekine H, Yajima Y. Alignment of biological apatite crystallites at first molar in human mandible cortical bone. *Cranio* 2012; 30: 32–40.
10. Furuya H, Matsunaga S, Tamatsu Y, Nakano T, Yoshinari M, Abe S, Ide Y. Analysis of biological apatite crystal orientation in anterior cortical bone of human mandible using microbeam X-ray diffractometry. *Mater Trans* 2012; 53: 980–984.
11. Mitsui T, Matsunaga S, Yamashita S, Nomoto S, Sato T, Abe S, Yoshinari M. Alignment of biological apatite crystallites in premolar and molar region in cortical bone of human dentate mandible. *J Hard Tissue Biol* 2016; 25: 233–240.
12. Merrot O, Vacher S, Merrot S, Godlewski G, Frigard B, Goudot P. Changes in the edentate mandible in the elderly. *Surg Radiol Anat* 2005; 27: 265–270.
13. Bassi F, Procchio M, Fava C, Schierano G, Preti G. Bone density in human dentate and edentulous mandibles using computed tomography. *Clin Oral Implants Res* 1999; 10: 356–361.
14. Alhassani AA, AlGhamdi AST. Inferior alveolar nerve injury in implant dentistry: diagnosis, causes, prevention, and management. *J Oral Implantol* 2010; 36: 401–407.
15. The McGill consensus statement on overdentures. *Quintessence Int* 2003; 34: 78–79.
16. Atwood DA, Coy WA. Clinical, cephalometric, and densitometric study of reduction of residual ridges. *J Prosthet Dent* 1971; 26: 280–295.
17. Devlin H, Horner K, Ledgerton D. A comparison of maxillary and mandibular bone mineral densities. *J Prosthet Dent* 1998; 79: 323–327.

18. Turkyilmaz I, Tözüm TF, Tumer C. Bone density assessments of oral implant sites using computerized tomography. *J Oral Rehabil* 2007; 34: 267–272.
19. Kingsmill VJ, Boyde A. Variation in the apparent density of human mandibular bone with age and dental status. *J Anat* 1998; 192: 233–244.
20. Wada H, Hosomichi J, Shimomoto Y, Soma K. Influence of occlusal hypofunction on the elastic property and bone formation of rat alveolar bone. *Orthod Waves* 2008; 67: 9–14.
21. Odaka K, Matsunaga S, Kasahara M, Nakano T, Yoshinari M, Abe S. Alignment of biological apatite crystallites in peri-implant bone of beagles. *Mater Trans* 2017; 58: 107–112.
22. Nakano T, Ishimoto T, Umakoshi Y, Tabata Y. Texture of biological apatite crystallites and the related mechanical function in regenerated and pathological hard tissues. *J Hard Tissue Biol* 2005; 14: 363–364.
23. Ishimoto T, Nakano T, Umakoshi Y, Yamamoto M, Tabata Y. Degree of biological apatite c-axis orientation rather than bone mineral density controls mechanical function in bone regenerated using recombinant bone morphogenetic protein-2. *J Bone Miner Res* 2013; 28: 1170–1179.
24. Inoue T. Dental implant-tissue response in situ-new pathema in wound healing-. *J Japanese Assoc Dent Sci* 1998; 17: 118–122.
25. Davies JE. Understanding peri-implant endosseous healing. *J Dent Educ* 2003; 67: 932–949.
26. Weber H, Morton D, Gallucci GO, Rocuzzo M, Cordaro L, Grütter L. Consensus

statements consensus statements and recommended clinical procedures regarding loading protocols. *Int J Oral Maxillofac Implants* 2009; 24: 180–184.

27. Iwata M, Matsunaga S, Morioka T, Nakano T, Abe S, Yoshinari M, Yajima Y. Alignment of biological apatite crystallites in posterior cortical bone of human edentulous mandible. *J Hard Tissue Biol* 2015; 24: 235–240.

Figure legends

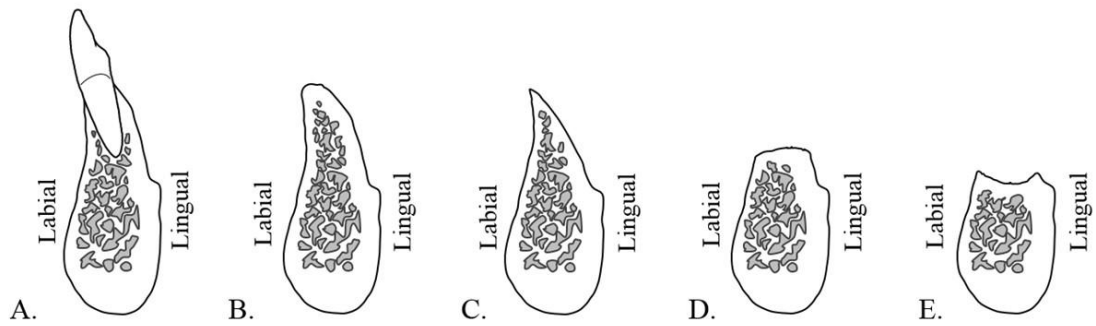


Fig. 1-A Schematic representation of sagittal sections in the five morphological categories.

A) Dentate mandible

B) Edentulous mandible with high, well-rounded alveolar region

C) Edentulous mandible with high, knife-edge alveolar region

D) Edentulous mandible with low, well-rounded alveolar region

E) Edentulous mandible with low, depressed alveolar region

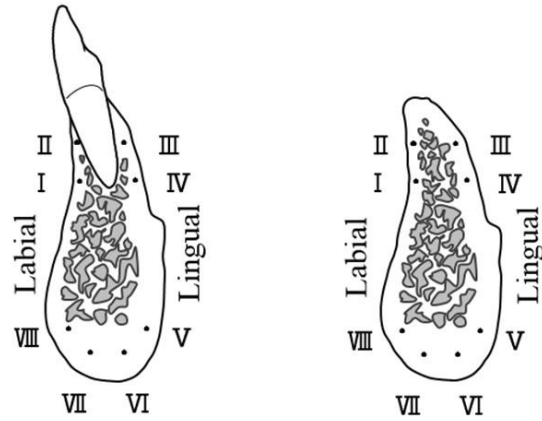


Fig. 1-B Measurement points on the mandible.

I, II: Alveolar region, labial side

III, IV: Alveolar region, lingual side

V, VI: Base of the mandible, lingual side

VII, VIII: Base of the mandible, labial side

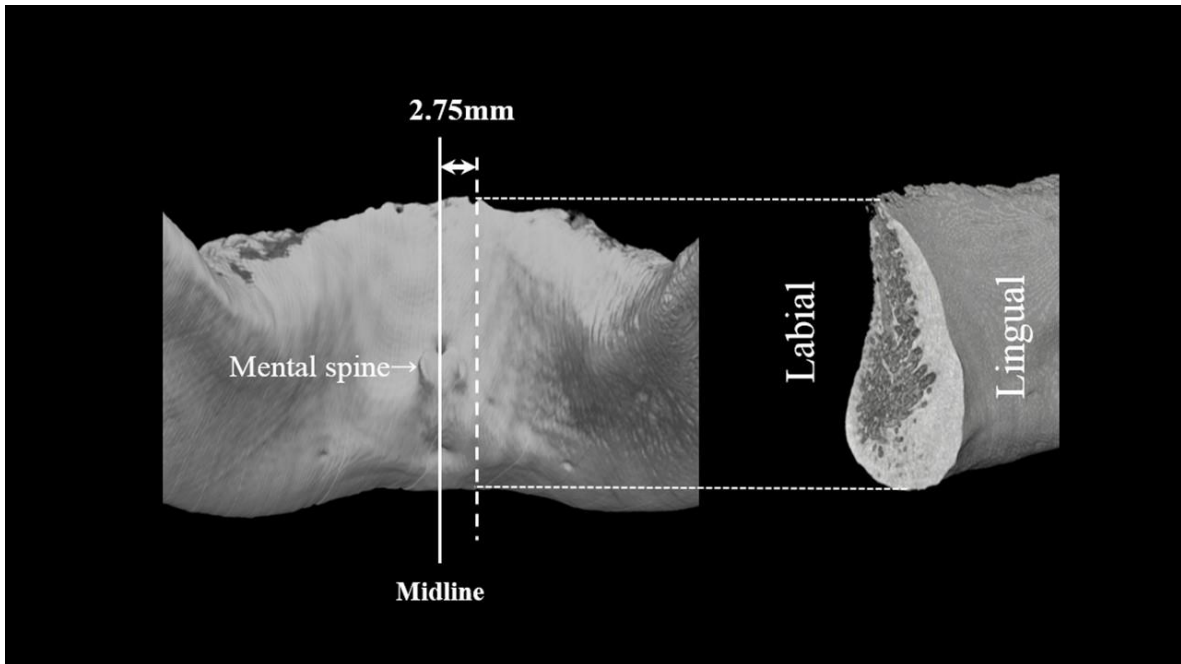


Fig. 2 Region of interest in the edentulous mandible. The region of interest was defined as a vertical section of the mandibular plane 2.75 mm from the midline, which was marked by the mental spine.

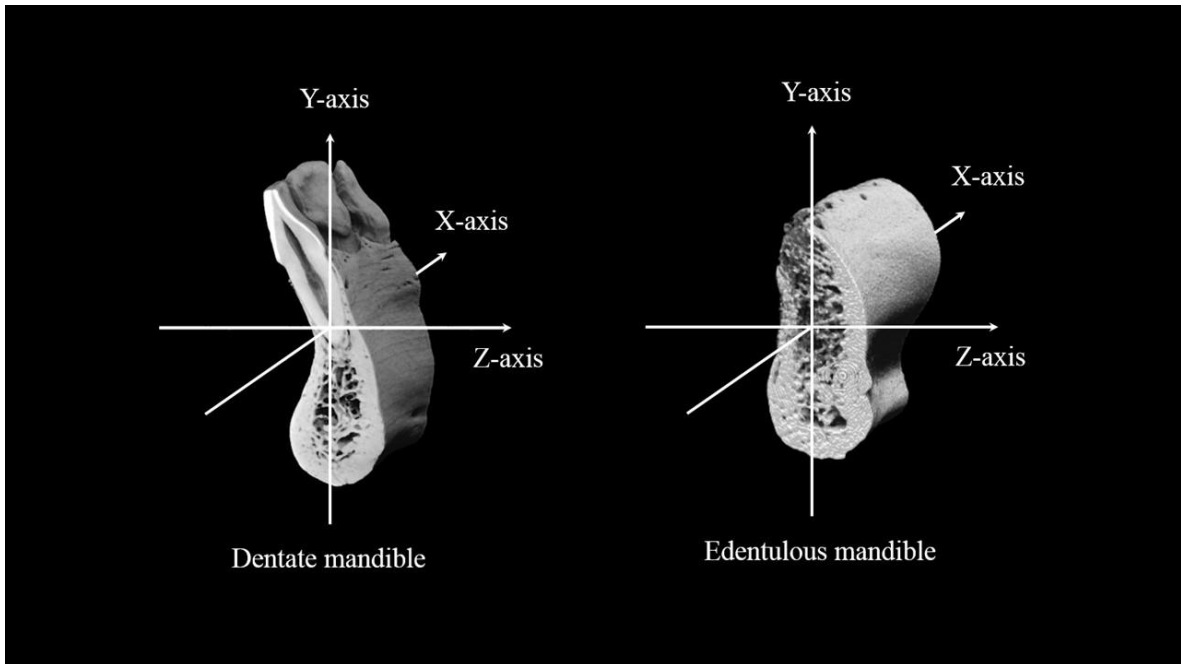


Fig. 3 Coordinate axes of the mandible. Three axes were established representing measurement direction. X-axis: mesiodistal direction. Y-axis: occlusal direction. Z-axis: labiolingual direction.

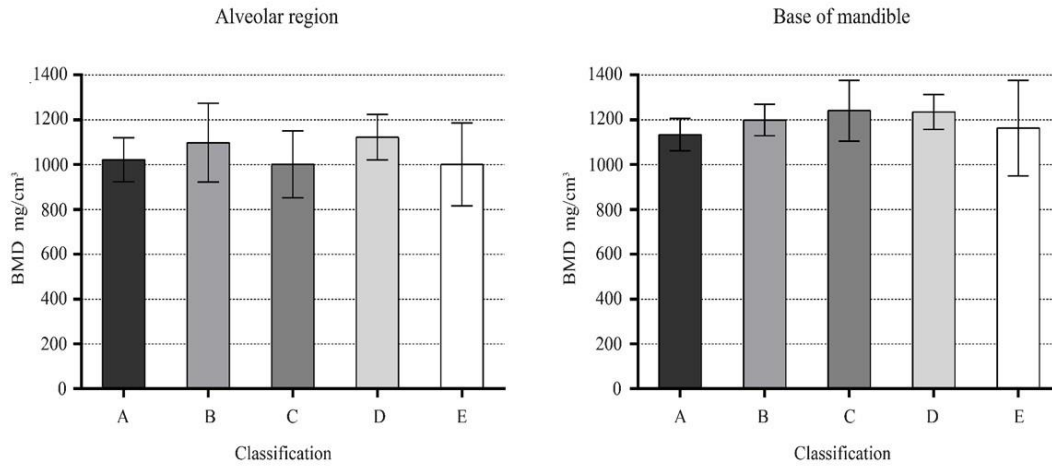


Fig. 4 Quantitative evaluation of BMD in the alveolar region and the base of mandible. BMD values (mg/cm³) are shown on the vertical axis and morphological categories on the horizontal axis. No significant differences in BMD were observed in the alveolar region or in the base of the mandible.

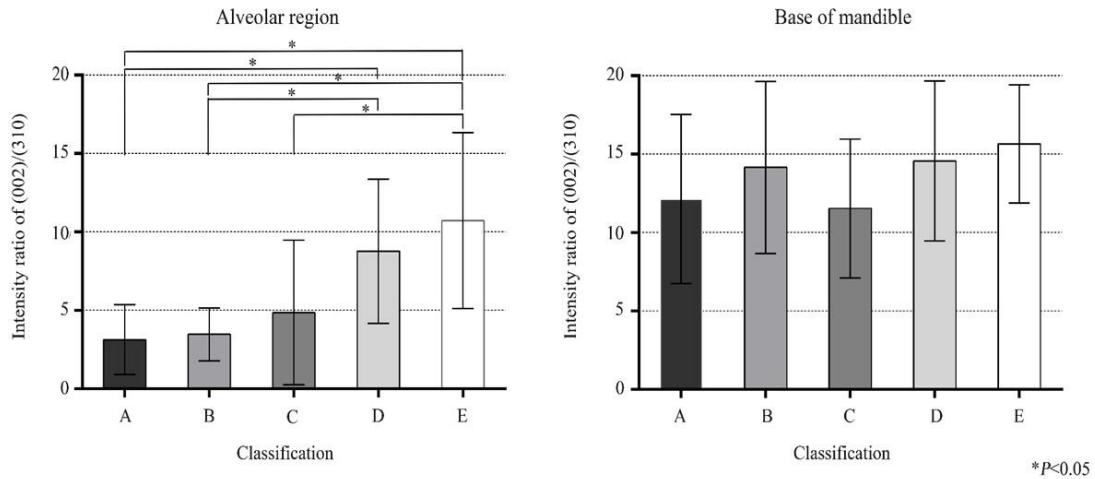


Fig. 5 BAp crystallite alignment in the alveolar region and the base of mandible in the X axis (mesiodistal) direction. Diffraction intensity ratios calculated from the (002)/(310) peaks are shown on the vertical axis and morphological categories on the horizontal axis. In the alveolar region, intensity ratios were significantly lower in categories A, B, and C compared to D and E. All ratios in the base of the mandible were high.

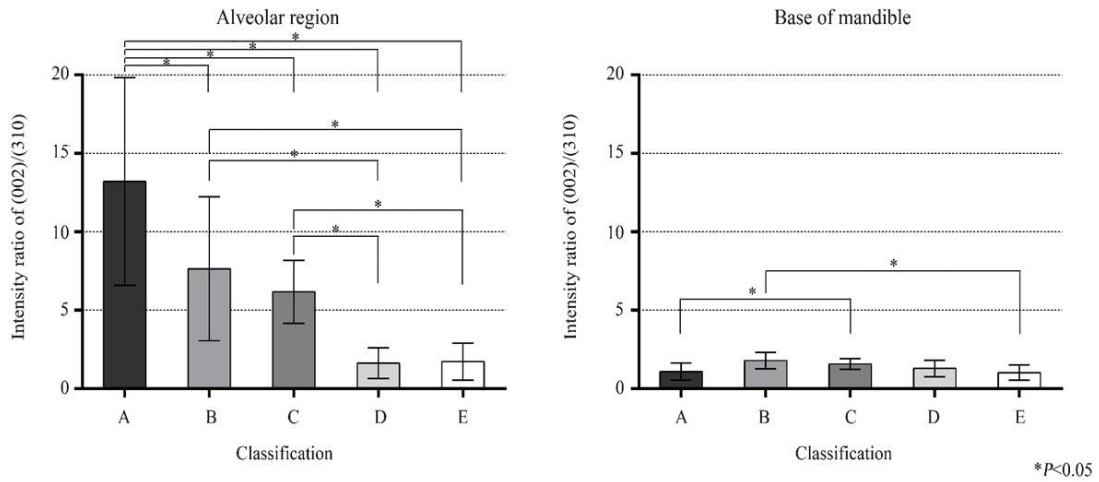


Fig. 6 BAp crystallite alignment in the alveolar region and the base of mandible in the Y axis (occlusal) direction. Diffraction intensity ratios calculated from the (002)/(310) peaks are shown on the vertical axis and morphological categories on the horizontal axis. In the alveolar region, intensity ratios were significantly higher in categories A, B, and C compared to D and E. All ratios in the base of the mandible were low.

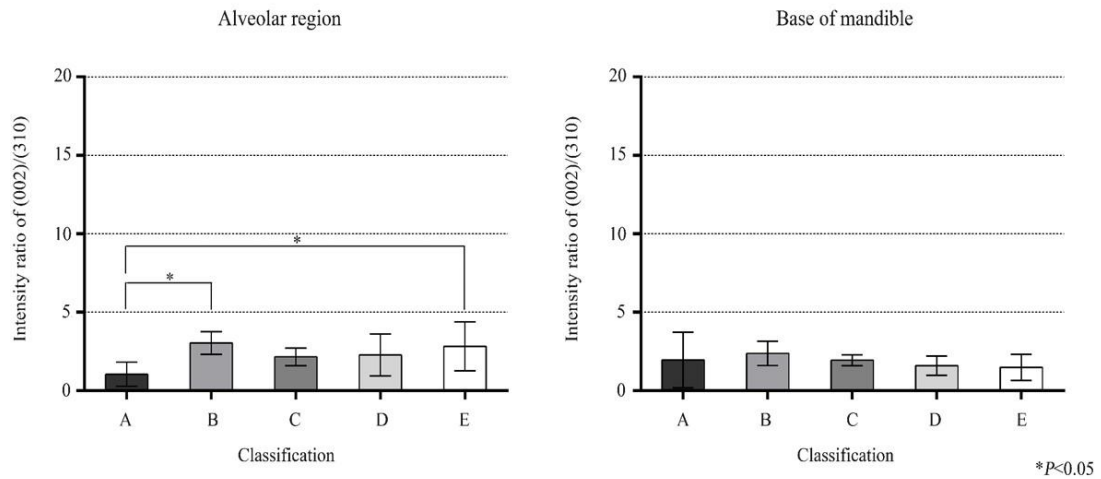


Fig. 7 BAp crystallite alignment in the alveolar region and the base of mandible in the Z axis (labiolingual) direction. Diffraction intensity ratios calculated from the (002)/(310) peaks are shown on the vertical axis and morphological categories on the horizontal axis. Intensity ratios were low in both the alveolar region and the base of the mandible.

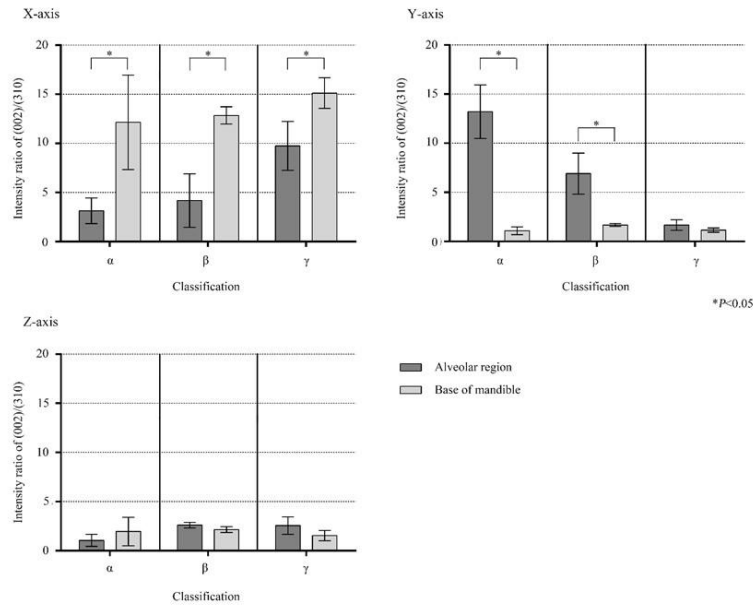


Fig. 8 BAp crystallite alignment in the alveolar region and the base of mandible depending on the extent of alveolar bone retention and resorption. The morphological categories were further grouped and compared as follows.

α: Dentate mandible (Category A).

β: Edentulous mandible with residual alveolar region (Categories B and C).

γ: Edentulous mandible with marked alveolar region resorption (Categories D and E).

Diffraction intensity ratios calculated from the (002)/(310) peaks are shown on the vertical axis and groups on the horizontal axis for the alveolar region and the base of the mandible. Significant differences in intensity ratios between the alveolar region and the base of the mandible were observed in the X and Y axis directions in groups α and β but only in the X axis direction in group γ.

Table 1 BMD (mg/cm³) at each measurement point.

Classification	Alveolar region				Base of mandible			
	I	II	III	IV	V	VI	VII	VIII
A	914.4	977.3	1095.3	1097.9	1144.1	1102.0	1172.4	1114.0
B	1097.2	1029.1	1133.5	1131.1	1212.3	1217.8	1208.4	1156.0
C	886.7	871.1	1124.9	1123.9	1220.2	1289.8	1279.4	1172.6
D	1070.0	1095.1	1129.8	1194.2	1234.5	1226.4	1258.5	1221.3
E	960.1	962.4	1005.2	1076.2	1180.0	1154.3	1173.7	1142.7

Table 2 X-ray diffraction intensity ratios in the X axis direction at each measurement point.

Classification	Alveolar region				Base of mandible			
	I	II	III	IV	V	VI	VII	VIII
A	1.49	3.58	4.59	2.87	12.91	8.15	18.65	8.87
B	2.29	3.01	3.10	5.51	13.95	15.22	14.72	12.77
C	2.64	1.84	4.16	10.83	14.30	10.01	9.59	12.27
D	4.21	6.18	12.06	12.63	16.02	13.66	13.94	14.63
E	11.29	11.16	6.34	14.09	18.67	14.40	14.18	15.40

Random aligned HAp powder (control): 1.5

Table 3 X-ray diffraction intensity ratios in the Y axis direction at each measurement point.

Classification	Alveolar region				Base of mandible			
	I	II	III	IV	V	VI	VII	VIII
A	15.18	11.66	10.19	15.82	1.07	0.82	1.64	0.82
B	9.30	10.78	5.03	5.46	1.66	1.82	2.03	1.64
C	8.03	6.74	4.89	5.01	1.73	1.30	1.73	1.55
D	2.43	1.82	1.29	0.96	1.01	1.11	1.40	1.63
E	0.68	3.08	1.60	1.55	0.88	0.95	1.46	0.81

Random aligned HAp powder (control): 3.0

Table 4 X-ray diffraction intensity ratios in the Z axis direction at each measurement point.

Classification	Alveolar region				Base of mandible			
	I	II	III	IV	V	VI	VII	VIII
A	0.45	1.53	1.61	0.59	1.06	1.59	1.04	4.11
B	3.10	2.72	3.56	2.79	2.22	2.61	1.67	3.02
C	2.87	2.35	1.62	1.77	1.86	1.94	1.96	2.01
D	2.65	2.35	2.65	1.45	1.51	1.68	1.10	2.07
E	4.75	1.96	2.82	1.78	1.50	1.00	0.96	2.48

Random aligned HAp powder (control): 3.0